Available online at www.CivileJournal.org

Civil Engineering Journal

(E-ISSN: 2476-3055; ISSN: 2676-6957)

Vol. 7, No. 03, March, 2021

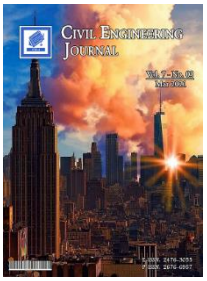

Computational Seismic Analysis of Dry-Stack Block Masonry Wall

Irfan Khan [1], Akhtar Gul [2*], Khan Shahzada [1], Nisar Ali Khan [3], Faisal ur Rehman [1], Qazi Samiullah [1], Muhammad Arsalan Khattak [1]

[1] *Department of Civil Engineering, University of Engineering and Technology, Peshawar, Pakistan.*

[2] *Department of Civil Engineering, University of Engineering and Technology, Bannu Campus-III, Pakistan .*

[3] *University of Roma Tre, Department of Architecture, Via Aldo Manuzio, 00153, Rome, Italy.*

Received 02 October 2020; Revised 10 February 2021; Accepted 18 February 2021; Published 01 March 2021

Abstract

In this research the computational modeling of Dry-Stack Block Masonry (DSM) walls subjected to cyclic monotonic loading testing is done. The analytical results were compared with experimental test results of the unreinforced and unconfined DSM cantilever walls subjected to lateral loading along with a constant axial load. ABAQUS has been used for Finite Element Modeling and analysis of the wall. Various material properties are defined for the wall in the software and modeled as a homogeneous material. The proposed numerical models had a good correlation with the experimental data. The test results discussion includes failure moods, load displacement curves, and stress/strain profile.

Keywords: Dry-Stack Block Masonry; Quasi-Static Test; ABAQUS; Concrete Damaged Plasticity.

1. Introduction

Masonry is the oldest structural typology of man-made construction material, dating back to 10000 BC. The standing monumental structures, buildings, bridges, palaces and towers in the world affirms the appropriateness of the material and methods [1].

Conventional masonry consists of units and binding materials. Cement-sand (CS) Mortar is a conventional binding material invented in the last two centuries when a construction revolution started to develop novel materials and methods. In the 19th century, after the invention of Portland cement, the conventional (CS) mortar replaced the old types of mortars. The performance and structural behaviour of masonry is influenced by the mechanical properties of mortar [2]. The past research studies revealed that the mechanical properties of CS mortar is not strong enough to resist the lateral forces, caused by large earthquake events [3]. The mortar often fails to serve as air or water tight against the external environment and differential settlement due to shrinkage when freshly placed. The compressive strength, tensile strength, water retentively, durability and bond strength of mortar are very important properties which led in modification in the basic proportions and constituents of CS mortar and/or additions.

Beside the poor structural behaviour and weak mechanical properties of conventional masonry, built with CS mortar has technological and workmanship drawbacks such as extra cost of bonding material, slow construction process, controlled workmanship difficulties [4]. Such limitations diverted the attention of researchers toward new

* Corresponding author: akhtarwazir@uetpeshawar.edu.pk

http://dx.doi.org/10.28991/cej-2021-03091668

methods and techniques of masonry construction which resulted in many new inventions in materials and methods. Dry stack masonry is one of the new technique developed in recent decades. Research reports revealed that the aforementioned difficulties and hurdles, related to CS mortar can be overcome by using dry stack masonry. In modern construction dry stacking is a relatively new mortar-less technology, but it is however based on the ancient construction technique. The dry stack masonry can be seen in ancient historical buildings in the form of dressed and undressed stone masonry. The Egyptians pyramids, Zimbabwe ruins (capital of Shona Kingdom) are the living example of dry-stack masonry [5, 6]. The invention of mud mortar, gypsum, lime, cement and Portland cement mortar replaced the use of dry-stack stone masonry and played an important role in the enhancement of mechanical properties of masonry. Since 1980, considering the aforementioned drawbacks in mortar, the researchers were compelled to considered the dry-stack masonry [4]. The conventional masonry based on CS mortar is now losing projects to the dry stack masonry [7].

In dry stacked masonry, the masonry units are laid without the use of mortar. Such technique is likely to give solutions to the mortar associated problems, including cost and construction duration of a project. Besides the construction benefits of the dry-stack masonry, its performance is satisfactory against lateral loads [4]. The cyclic loading on dry-stack masonry showed that the deformation and energy dissipation capacity of dry-stack masonry is not significantly affected by the high strength of units [8].

In order to analyse the behaviour of existing structure and /or to assess models with new material and methods, it is necessary to develop numerical tools and procedures which will preserve the physiognomy of structures. The most commonly used numerical tool for masonry analysis is the finite element method, wherein the material is modelled as a homogeneous orthotropic continuum, while the dry masonry is modelled by discrete element method. Numerical modelling of dry-stacked masonry structures is an efficient technique to analyse and examine its structural behaviour. Numerous research work has been carried out on the computational behaviour of conventional masonry, but little research work has been done, to analyse numerically, the in-plane behaviour of DSM. Experimental research work gives an actual testing data and graphical representation of a structural behaviour but is time consuming, laborious and uneconomical. Therefore, this research work has been carried out to analyse the dry-stack block masonry walls for in-plane behaviour, using numerical strategy.

Various modelling approaches have been used to analyse the behaviour of masonry structures. The three modelling strategies suggested by Lourenco (1996) [9] are micro-modelling, meso modelling, and macro-modelling. This author further added that meso modelling only deals with the interface bond strength between masonry units through mortar while the behaviour of mortar itself is not considered. Micro-modelling requires high computational efforts as the masonry units are modelled one by one, while macro-modelling is a homogeneous model and requires less computational efforts [10].

Micro-modelling of DSM wall was performed by using DIANA as an eight node continuum plane stress element, while joints are modelled as a six node and zero thickness line interface [11]. The experimental and numerical behaviour matched for monotonic load while the same did not match for cyclic loading because of crack closure.

Ample research work has been carried out on the computational behaviour of conventional masonry, but little research work has been done, to analyse numerically, the in-plane behaviour of dry-stack masonry. Experimental research work gives an actual testing data and graphical representation of a structural behaviour but is time consuming, laborious and uneconomical. Therefore, this research work has been carried out to analyse the dry-stack block masonry walls for in-plane behaviour, using numerical strategy.

In this research work an analytical attempt has been made to model an unconfined/unreinforced DSM wall, using finite element package ABAQUS. The analytical results thus obtained have been compared with the experimental results to check the authentication of the numerical tool. The in-plane behaviour of dry-stacked masonry wall with pre-compression loading has been assessed numerically for principal stresses and strains, tensile and compression damages.

2. Method and Numerical Modeling

It is essential to know the behaviour of the DSM wall, under lateral loading conditions so that the influence of various factors can be predicted. It is laborious and costly to perform experimental work for various loading with various materials and methods. Hence, computer modelling procedures have been tried in this research work for modeling DSM walls, which compensates the above-described drawbacks of experimental scheme. A Finite Element (FE) model has been developed to produce a numerical approach, compatible with experimental results, in order to develop a better understanding of the structural behaviour of DSM. The Flowchart for the 3D Finite Element Modelling (F.E.M) of the wall is shown in Figure 1.

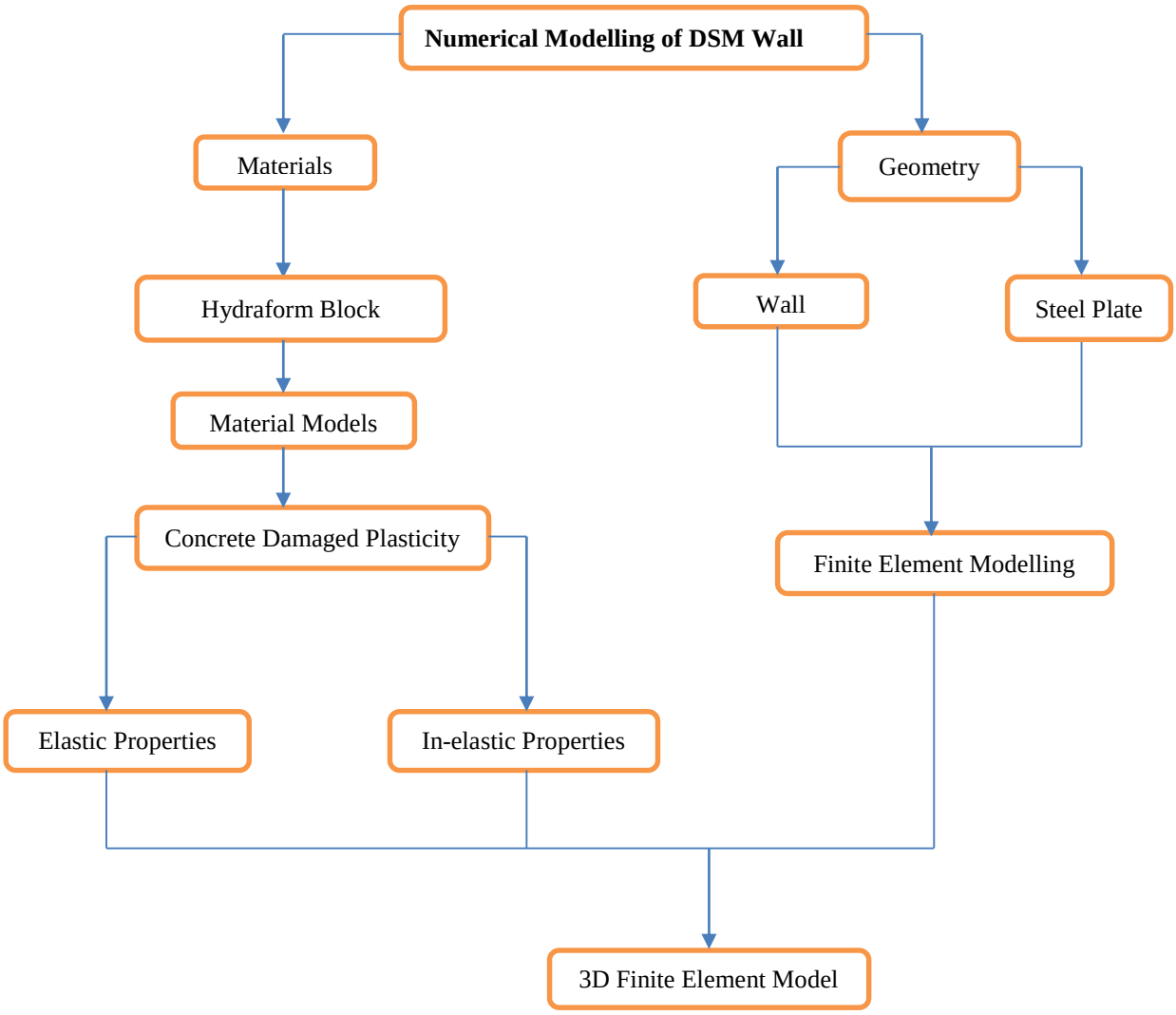

Figure 1. Flowchart for the 3D finite element model of the wall

2.1. Description of the Wall

The numerical model has been developed, using ABAQUS/CAE for the experimental tests and data performed on DSM in the Structural Laboratory of University of Engineering and Technology Peshawar. Three piers were tested under quasi-static loading with aspect ratio of 1.02. The DSM walls have dimensions of 58″ (1468 mm)*57″ (1448 mm)*8.5″ (215.9 mm). The experimental setup of the wall is shown in Figure 2.

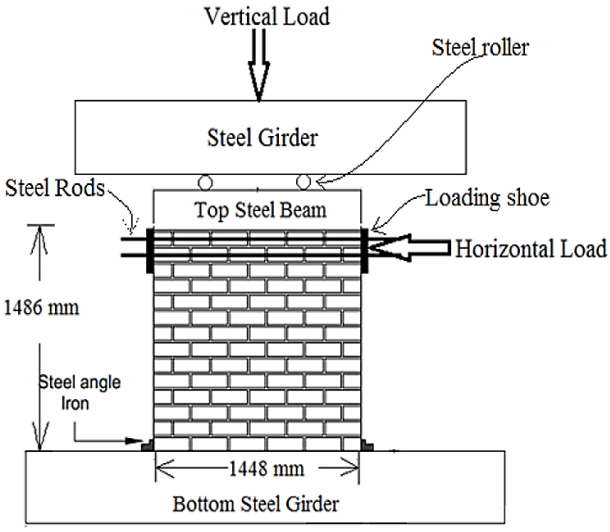

Figure 2. Experimental Setup of the Wall

2.2. Numerical Modeling using ABAQUS

ABAQUS is a multi-dimensional numerical tool in which, both linear and nonlinear FE analysis can be performed. It has extensive material and element libraries, which can model virtually any geometry with various analysis procedures [12]. For the analysis of the DSM wall, ABAQUS includes material models that can be used, to define the elastic and plastic properties of the block. Two parts were defined for modelling the wall; the masonry wall and loading shoe, on which lateral displacement is applied. The loading shoe was tied to the top lateral side (thickness) of the wall. There are different systems of units in ABAQUS. In this case, BIN (lb-in-sec) was used as a system of units. The 3D Model of F.E Geometry of the wall for monotonic and cyclic load is shown in Figure 3 (a and b) respectively.

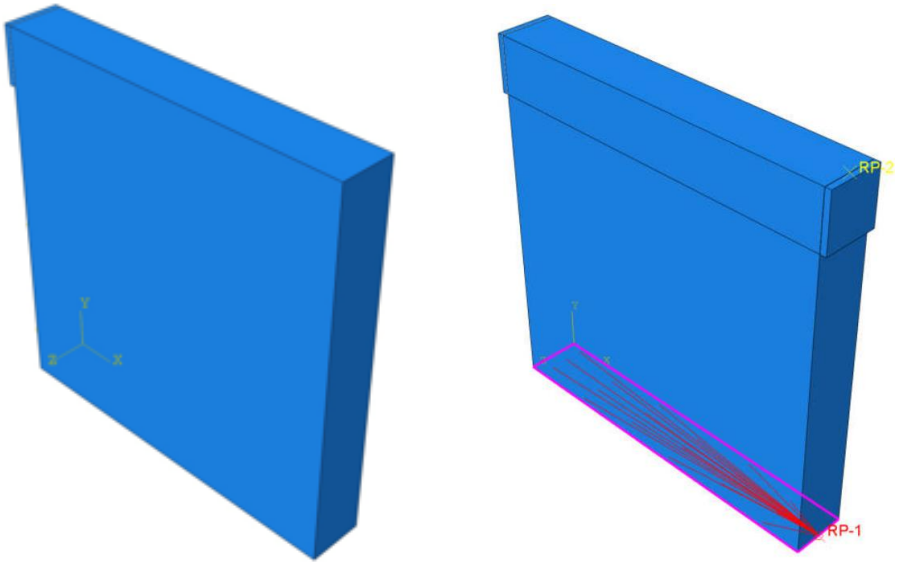

(a) (b)

Figure 3. (a) Model with single steel plate for monotonic load (b) Model with two steel plate for cyclic load

2.3. Material Models

Material models have been developed to examine the structural behaviour of the Hydraform block material. Concrete Damage Plasticity (CDP) Model is used for the analysis because the CDP provides permanent effects of damages occurring in the material due to low restraining pressure. The CDP works on masonry (brick or concrete, etc.) and other quasi-brittle materials, subjected to cyclic and dynamic lading.

2.3.1. Material Properties in CDP

In CDP, the following properties were found for the tested wall material;

Elastic Properties

The elastic properties of the masonry wall have been tabularized in Table 1, obtained from experimental work.

Table 1. Elastic Properties of DSM

Property	Value
Density (lb/ft^3)	132
Modulus of Elasticity (ksi)	606.66
Poisson Ratio	0.2

Inelastic Properties

Plasticity: For plastic behaviour of the masonry, parameters given in Table 2 have been incorporated after several trials, starting with default values as input in ABAQUS.

Table 2. Plasticity Factors

Dilation Angle (degree)	Eccentricity	f_{b0}/f_{c0}	K	Viscosity Parameter
45	0.1	1.3	0.5	0

Compressive Behaviour: The ultimate compressive strength of masonry prism obtained from the experimental results is used for the numerical analysis. The stress-strain curve of the experiment is given in Figure 4:

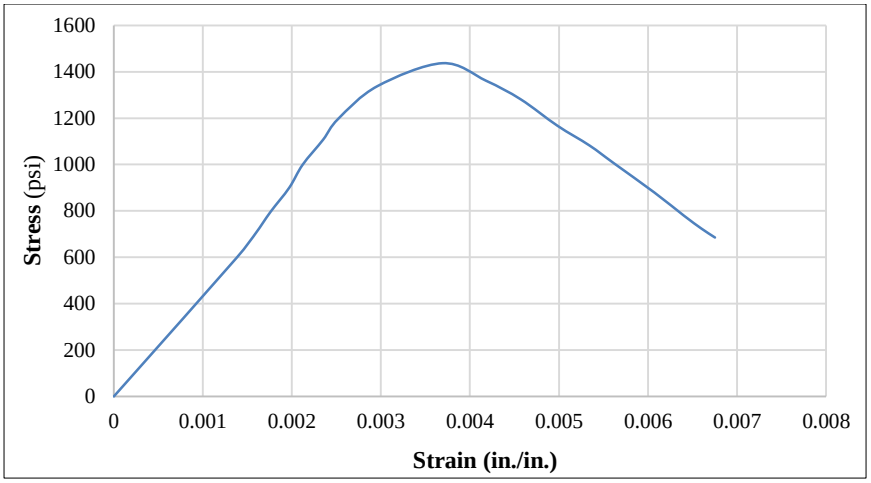

Figure 4. Compressive stress-strain curve

The inelastic strains are calculated using Equation 1 [13]:

$$\varepsilon_{in} = \varepsilon_t - \varepsilon_{el} \quad (1)$$

Where, ε_{in} denotes "Inelastic strain", ε_t "Total strain" and ε_{el} "Elastic strain". The damage parameter is used to find damages in the walls after peak load. It is calculated by Equation 2 [13]:

$$d_c = 1 - {}^{\sigma_c}/_{\sigma_c'} \quad (2)$$

Where *dc* denotes the damage parameter in compression, σ_c the compressive strength of masonry after peak stress and σ'_c the ultimate compressive strength of masonry.

The plastic strain is calculated by Equation 3:

$$\varepsilon_c^{pl} = \varepsilon_c^{in} - \frac{d_c}{1 - d_c} \cdot \frac{\sigma_c}{E_0} \quad (3)$$

Equation 1 to Equation 3, graphically are shown in Figure 5.

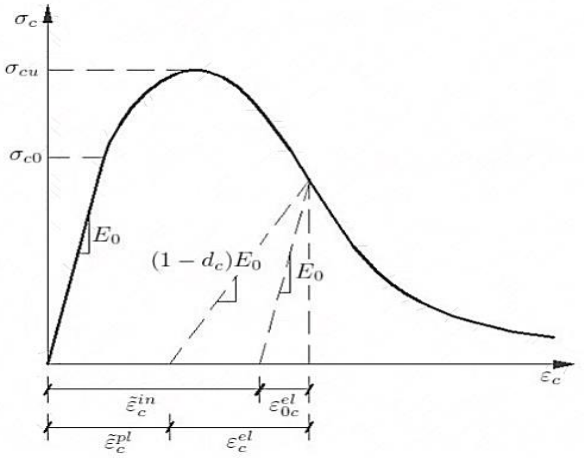

Figure 5. Demonstration of Compressive Inelastic Strains [17]

Tensile behaviour

The ultimate tensile strength of DSM wall for bending in longitudinal direction is 14.5 psi [14] but taking this value the result doesn't match with the experimental result. At 20 psi both the results match satisfactorily. This may be because of the frictional forces between the surfaces of the blocks, defined by the Equation used by Deepak (2010) [14]. In masonry, the tensile stress values vary linearly from zero to peak value and then start decreasing exponentially. From ultimate value of tensile stress, the strain is calculated using Equation 4 [15, 16];

$$\sigma_t^1 = E_c \varepsilon_t \quad (4)$$

The second part (exponential) of the curve is calculated using the relation 5 [15, 16]:

$$\sigma_t^2 = f_{cr} (\frac{\varepsilon_{cr}}{\varepsilon_t})^c \quad (5)$$

The tensile stress-strain plot of the material is shown in Figure 6.

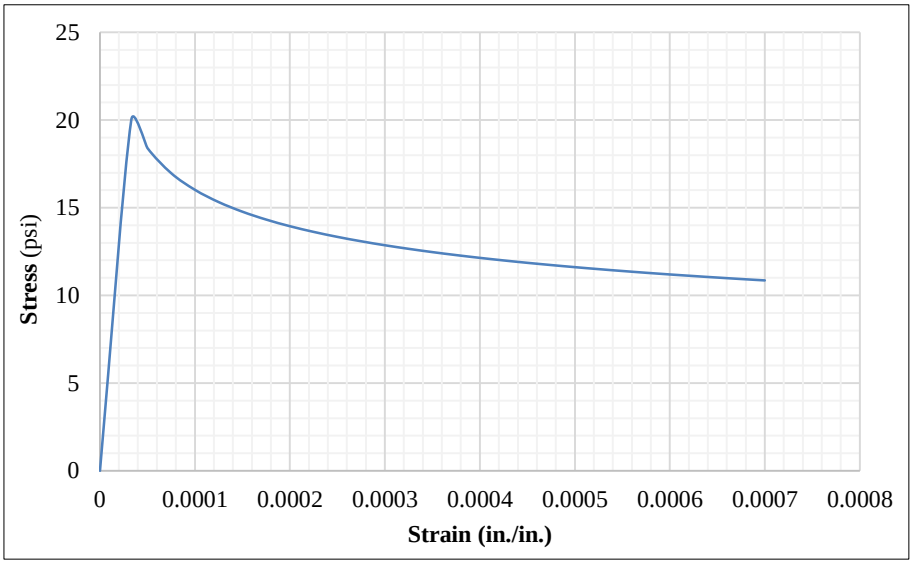

Figure 6. Tensile stress-strain curve

The cracking strains are calculated using Equation 6.

$$\varepsilon_{cr} = \varepsilon_t - \varepsilon_{el} \tag{6}$$

Where, ε_{cr} denotes cracking strain. The damage parameter is calculated by Equation 7;

$$d_c = 1 - {\sigma_t}/{\sigma_t'} \tag{7}$$

The plastic strain is calculated by Equation 8:

$$\varepsilon_t^{pl} = \varepsilon_t^{in} - \frac{d_t}{1 - d_t} . \frac{\sigma_t}{E_0} \tag{8}$$

The Equations 6 to 8 are graphically shown in Figure 7. There is a significant difference in the exponential part between the actual and analytical graphs. The exponential portion depends on the parameters used in Eqn. 5. In this case, the behaviour was accurately predicted by Figure 7.

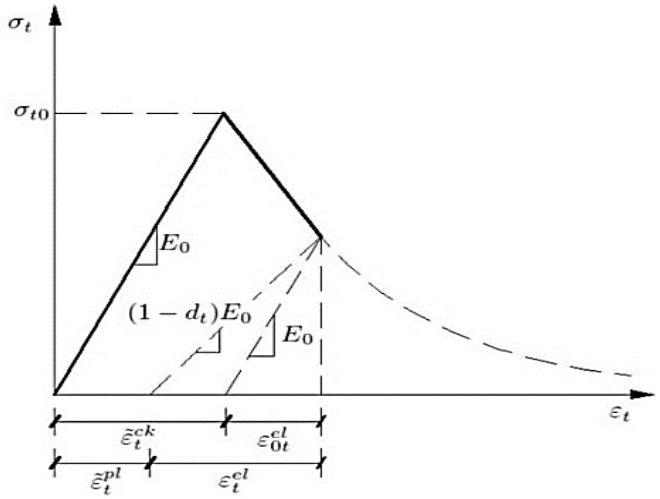

Figure 7. Definition of Tensile Inelastic Strains [17]

The model is initially in compression under the Pre-Compression step and then propagates it through DispCont till its end. The Pre-compression stress of 58 psi (equal to the effect of two-story load) was placed with "Ramp Amplitude" and lateral displacement of 8 mm (0.314 in.) was applied for monotonic response. For cyclic loading, the lateral displacement was applied as 2 mm, 4 mm, 6 mm and 8 mm, with each applied in the negative direction. In addition to default output variables, two outputs were added to output variables; one for x-directional reactions at the bottom of the wall at the reference point (RP-1) and the second for displacement in the x-direction at the top of the wall, denoted as U1. Figure 8 (a and b) shows the model with monotonic and cyclic lateral displacement respectively.

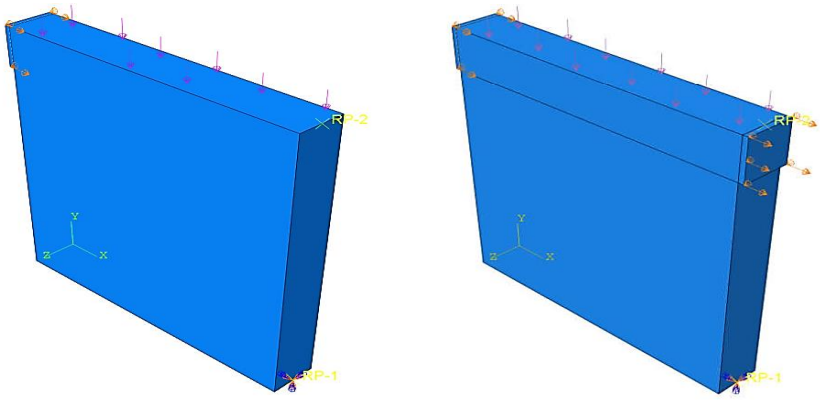

(a) (b)

Figure 8. (a) Model with pre-compression load and lateral monotonic displacement (b) Model with pre-compression load and lateral cyclic displacement

3. Results and Discussion

3.1. Monotonic Behaviour

The analysis was run using "Job Module". After the analysis was done, the model was envisioned via "Visualization Module". The X-Y plots were obtained and matched with respect to four performance levels as per [18], shown in Figure 9. Performance Levels have been selected because they have readily identifiable consequences associated with the post-earthquake disposition of a building that is meaningful to the building community. These include the ability to resume normal functions within the building, the advisability of post-earthquake occupancy, and the risk to life safety.

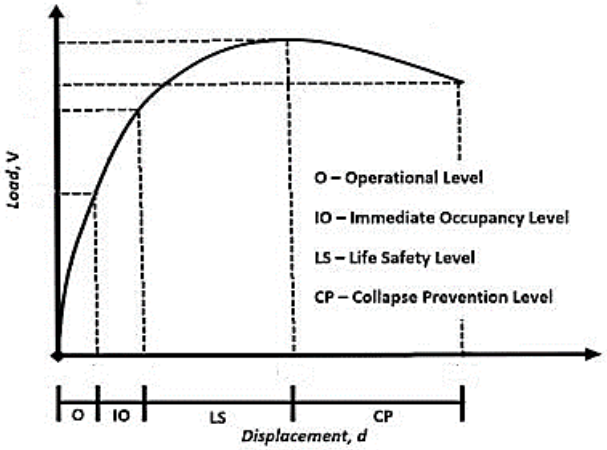

Figure 9. Performance Levels [18]

The Load-Deformation curve obtained from the result is shown in Figure 10.

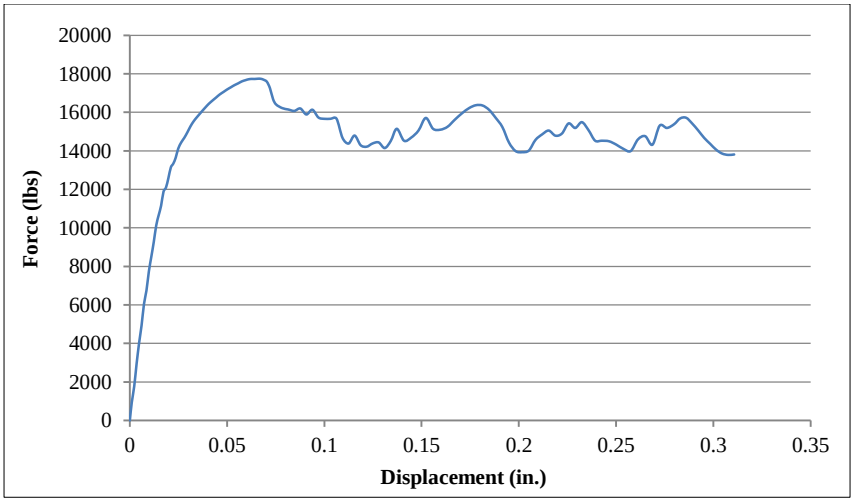

Figure 10. Load-Deformation plot of the Model (Unidirectional load)

The tension damage initiated at 0.025 inch deformations at which the sideways load was 8000 lbs. This state is associated with Operational Level (O) performance. At a displacement of 0.045 inches, significant tension damage appeared at the center of the model, at which the corresponding lateral load was 16000 lbs. This state is linked to the Immediate Occupancy "IO" level. At 0.07 inch displacement, significant cracks appeared, at which the corresponding lateral load value was 17696.36 lbs. The peak lateral load is 17696.36 lbs and is linked to the Life Safety "LS" level. The peak displacement at which analysis was stopped was 0.314 inches, at which lateral load correspondingly was 13817.18 lbs. This level of performance is linked to Collapse Prevention "CP" level.

3.1.1. Comparison with the Experimental Data

The Figure 11 shows the comparison between experimental and numerical graph. From the Figure, it is clear that both the experimental and numerical graph matches perfectly in linear part. But the lateral displacement reaches to the ultimate value (0.314 in.) in numerical case, while in case of experimental result it reaches "0.275 in."

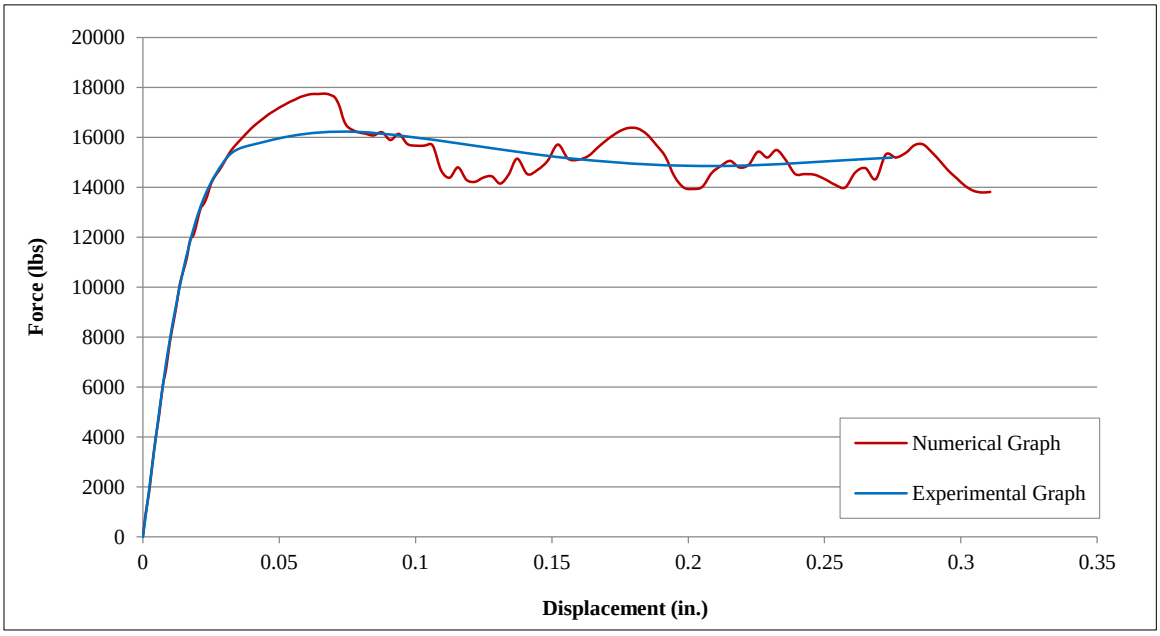

Figure 11. Comparison of Experimental and Numerical results

The same was performed by Senthivel and Lourenço (2009) [19] monotonic analysis on dry stone masonry for various pre-compression loadings.

3.1.2. Stress-Strain Visualization

Stress-strain contours (consisting of misses stresses and plastic strains) obtained from the results are presented for the aforementioned performance levels. In Figure 12, Misses stresses at each level are shown.

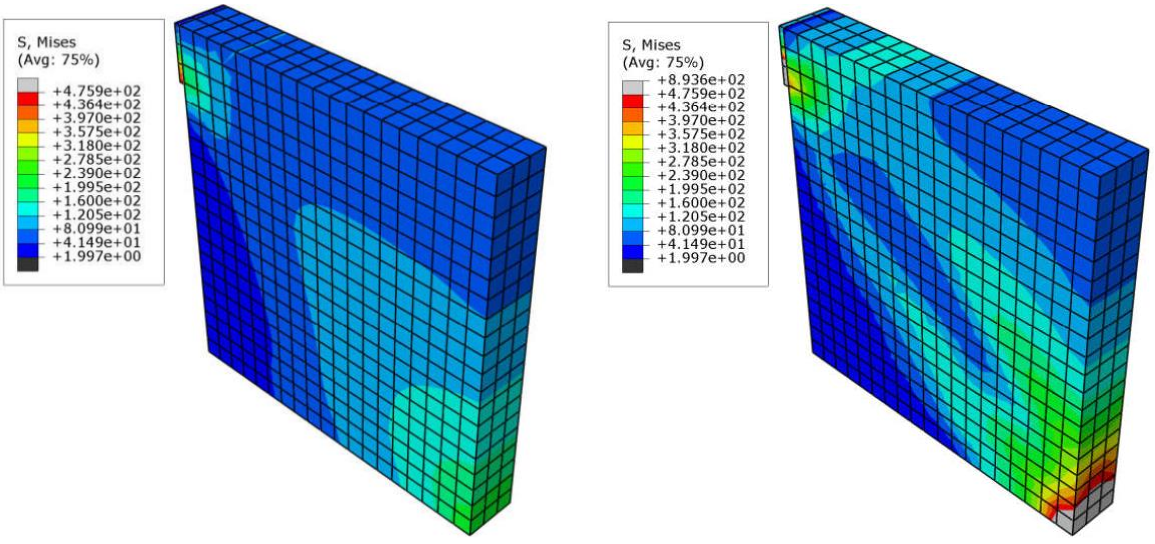

(a) (b)

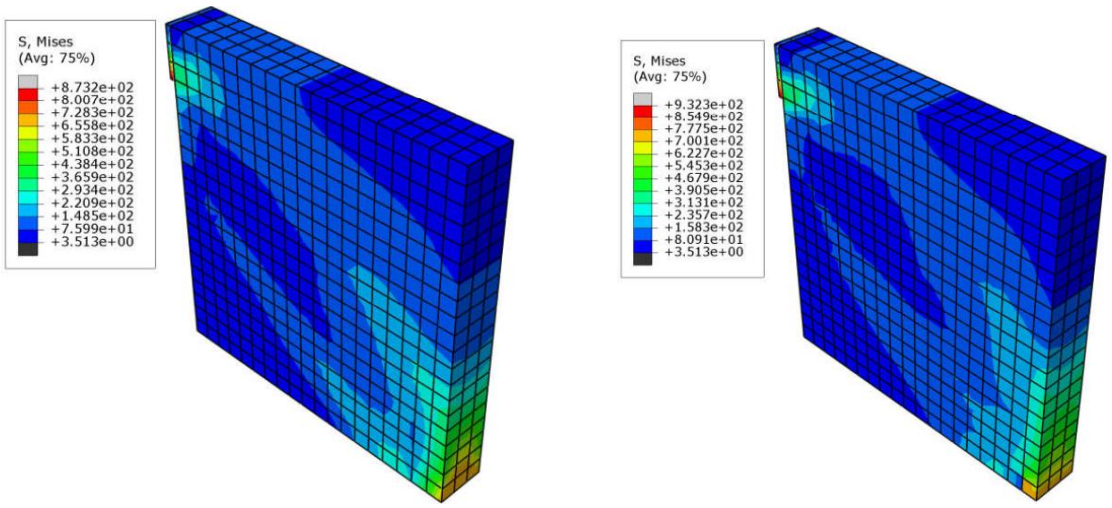

(c) (d)

Figure 12. (a) Misses Stress at Operational Level (b) Misses Stress at Immediate Occupancy level (c) Misses Stress at Life Safety level (d) Misses Stress at Ultimate Limit State (Collapse Prevention level)

The maximum principal stresses on the wall at different performance levels are shown in Figure 13. The principal strains at the operational level start at the rocker point; at the immediate operational level, the crack begins at the corner opposite to the lateral displacement point, propagates diagonally up to the collapse prevention level.

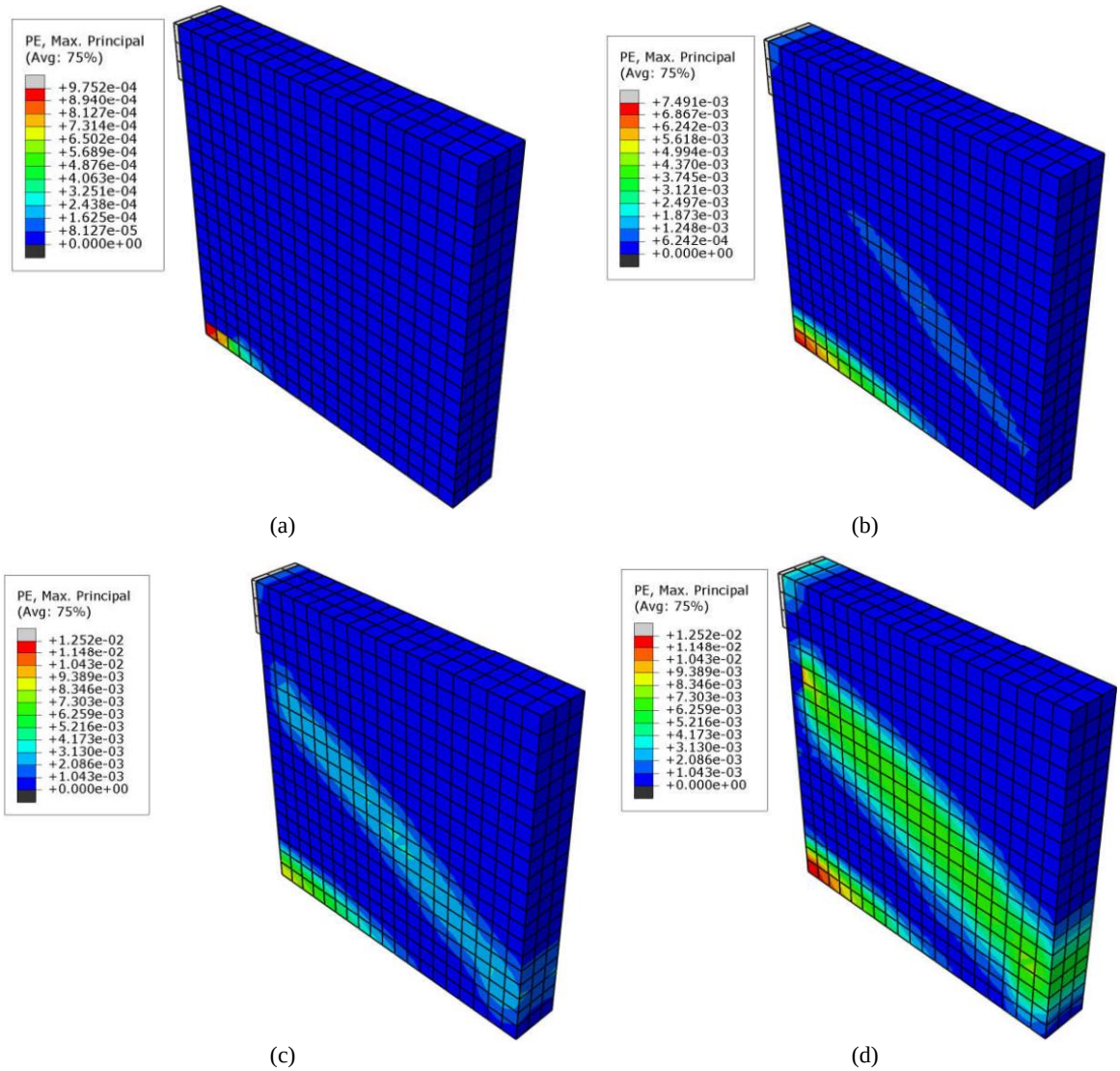

(a) (b)

(c) (d)

Figure 13. (a) Max. Principal Plastic Strains at Operational level (b) Max. Principal Plastic Strains at Intermediate Occupancy level (c) Max. Principal Plastic Strains at LS level (d) Max. Principal Plastic Strains at CP level

The same maximum principal strains were also observed by Annecchiarico et al. (2010) and Rafiq (2016) [20, 21] for brick wall considering homogeneous in ABAQUS.

3.1.3. Damage Visualization

This section displays damages at each performance level in Figure 14. As masonry is weak in tension, significant damages in tension are observed. Being strong in compression, minor crack is observed at the ultimate level, as shown in Figure 15.

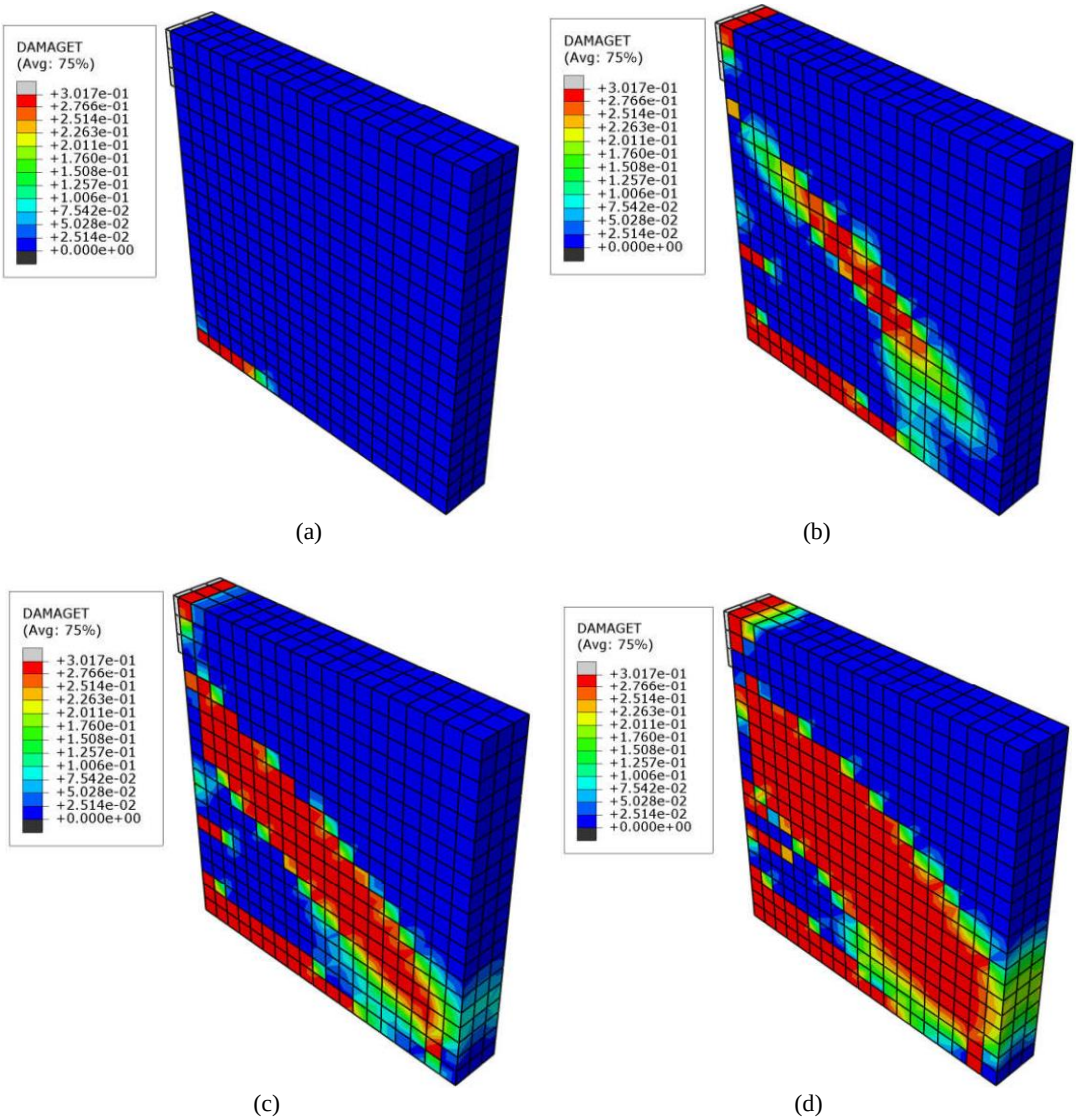

Figure 14. (a) Tension Damage at Operational Level (b) Tension Damage at IO level (c) Tension Damage at Maximum Resistance (LS level) (d) Tension Damage at Ultimate State

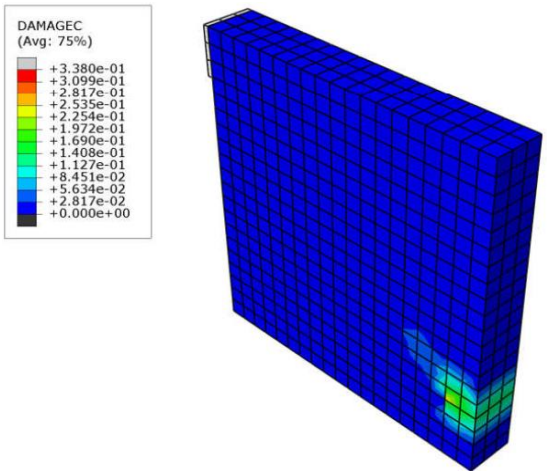

Figure 15. Compression Damage at Ultimate State (CP level)

The visual comparison of the cracks is shown in Figure 16.

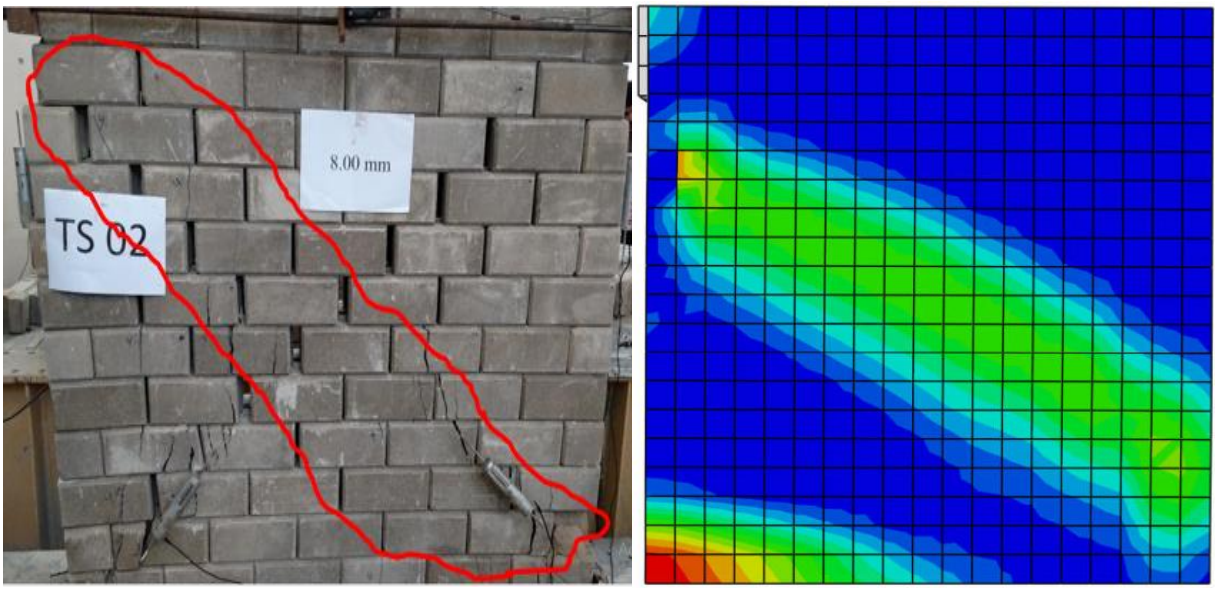

Figure 16. Cracks comparison between experimental and numerical work for monotonic load

The same pattern was observed by Nikolić et al. (2016) [22] during the numerical behaviour of Dry Stone Masonry. Similarly Kadhim and Dawood (2020) [26] observed cracks in both confined and unreinforced clay brick masonry models using ANSYS.

3.1.4. Parametric Study

Increase in Pre-compression loads

By increasing the pre-compression load, the lateral load resistance increases as shown in Figure 17, for various pre-compression loads. The same situation was observed experimentally by Safiee et al. (2011) [23] during the investigation of the in-plane behaviour of interlocking dry masonry walls.

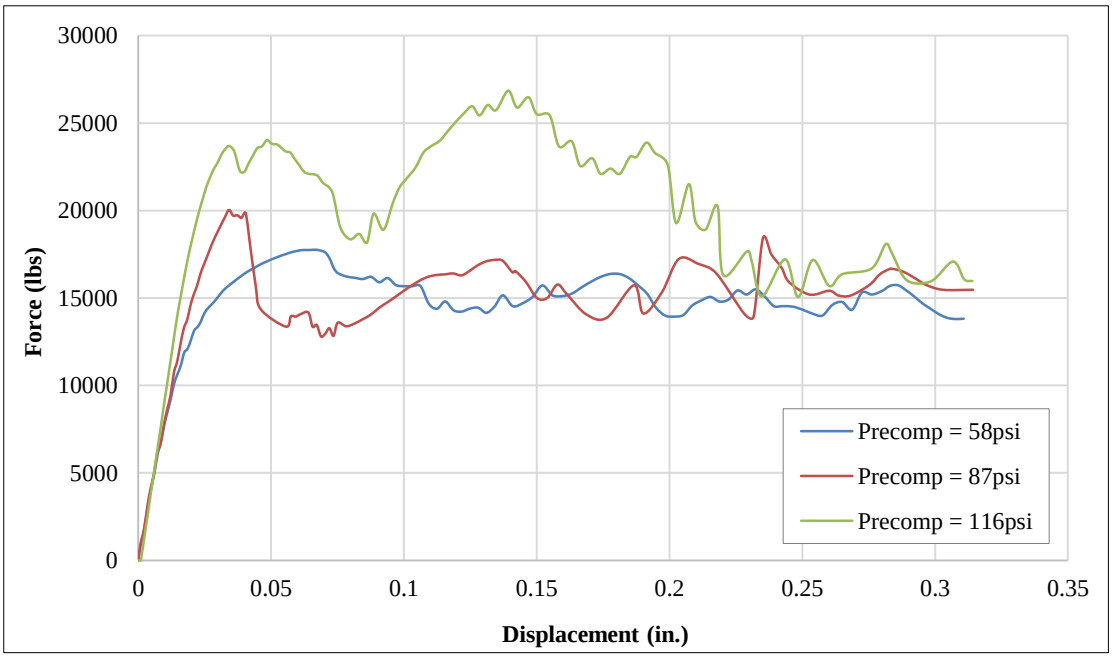

Figure 17. Load-Deformation graph for different pre-compression loads

Change in Aspect Ratio

The height to length ratio of a wall has great effect on its in-plane behaviour. When the height of a wall increases, the stiffness and lateral load capacity decreases, as shown in Figure 18. From Figure 18, it is clear that when the aspect ratio is increased, the peak load goes on decreasing while the peak lateral displacement increases, which was also

observed by Abdi et al. (2018) [24]. This shows that the wall with higher aspect ratio reaches ultimate displacement in elastic state, while the wall with low aspect ratio covers much plastic stage up to the ultimate lateral displacement. The wall with high aspect ratio has low stiffness as compared to the wall with low aspect ratio. This expression is in close agreement, presented by Iuorio et al. (2012) [25].

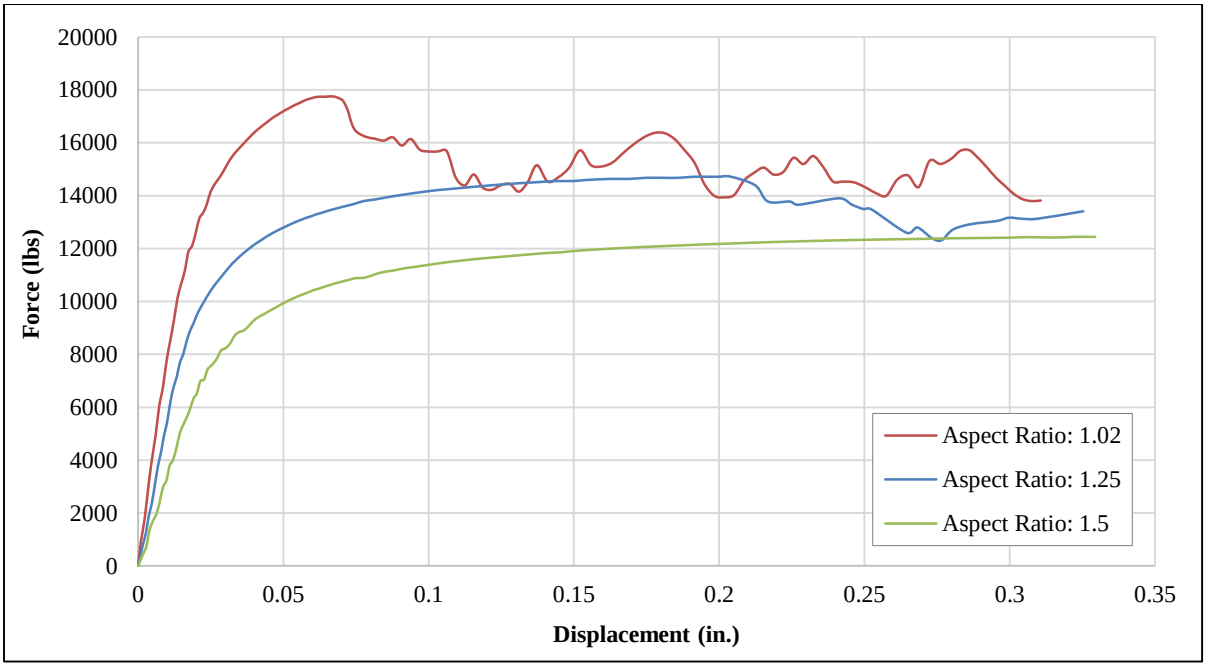

Figure 18. Load-Deformation behaviour for the two aspect ratios

3.1.4.3 Cyclic Behaviour

The load deformation graph of the cyclic loading is shown in Figure 19. The hysteresis loops of cyclic loading is in "S" shape while in this analysis the shape is not resemblance to S, which is due to, not assuming several non-linear properties in ABAQUS.

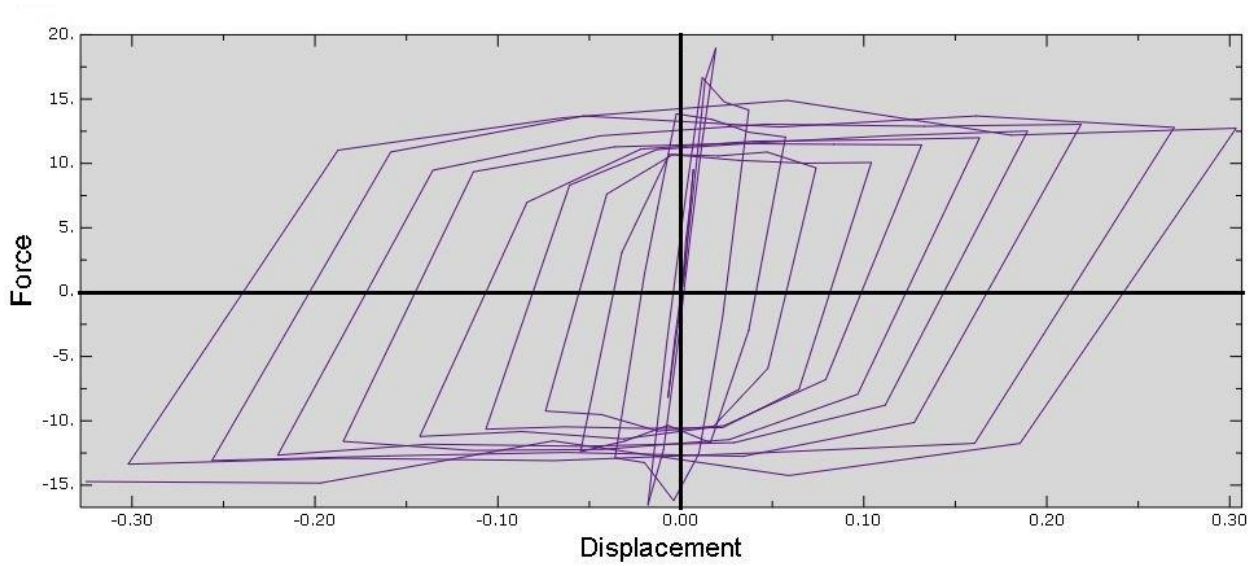

Figure 19: Load (kips)-Deformation (in.) graph of the model subjected to cyclic loading

4. Conclusions

This numerical investigation was done on the experimentally tested wall, and the conclusions of the study can be summarized as follows;

The results obtained from experimental work and numerical analysis using ABAQUS, of DSM walls showed a well-defined similarity in behaviour in the elastic range. The damage patterns of experimental and numerical model for monotonic lateral displacement are closely matching, which shows the authenticity of the Finite Element Package.

The monotonic response of multi-story DSM can be predicted accurately based on the results of the ABQUS software. Though the pattern of Hysteresis loop, obtained from ABAQUS does not accurately match with the experimental plot, yet the cyclic behaviour of DSM can be predicted. The plastic strains match with the corresponding experimental diagonal cracks for cyclic loading.

5. Declarations

5.1. Author Contributions

All authors contributed to the design and implementation of the research, analysis of the results and writing of the manuscript. All authors have read and agreed to the published version of the manuscript.

5.2. Data Availability Statement

The data presented in this study are available in article.

5.3. Funding

The author(s) received no financial support for the research, authorship, and/or publication of this article.

5.4. Conflicts of Interest

The authors declare no conflict of interest.

6. References

[1] Kömürcü, Sedat., Analysis and Modelling of the in-plane behaviour of Masonry Walls, PhD Thesis, Istanbul Technical University, Turkey (2017).

[2] De C.S.S. Alvarenga, Rita, Gustavo H. Nalon, Lucas A. F. Fioresi, Monica C. Pinto, Leonardo G. Pedroti, and José C. L. Ribeiro. "Experimental Evaluation of the Influence of Mortar's Mechanical Properties on the Behavior of Clay Masonry." The Minerals, Metals & Materials Series (2017): 671–679. doi:10.1007/978-3-319-51382-9_74.

[3] Messali, F., R. Esposito, G. J. P. Ravenshorst, and J. G. Rots. "Experimental Investigation of the in-Plane Cyclic Behaviour of Calcium Silicate Brick Masonry Walls." Bulletin of Earthquake Engineering 18, no. 8 (April 5, 2020): 3963–3994. doi:10.1007/s10518-020-00835-x.

[4] Ngowi, Joseph Vincent. "Stability of dry-stack masonry." PhD Thesis, University of the Witwatersrand, Johannesburg, South Africa. (2005).

[5] Walker, P.J, Maunsel, M.G and Dickens, J.G., Structural Instability at Great Zimbabwe Monument, research report, University of Zimbabwe (1991).

[6] Uzoegbo, H.C., Stabilised soil blocks; Properties and Applications, Technical notes, Dept. of Civil Eng., University of Witwatersrand (2000).

[7] Vanderwerf, P., Mortarless Block Systems analysis of systems in the market, Works Inc. new construction products report, Stoughton (1999).

[8] Lin, Kun, Yuri Totoev, Hongjun Liu, and Chunli Wei. "Experimental Characteristics of Dry Stack Masonry under Compression and Shear Loading." Materials 8, no. 12 (December 12, 2015): 8731–8744. doi:10.3390/ma8125489.

[9] Lourenco, P.B., Computational Strategies for Masonry Structures, PhD thesis, Delft University of Technology, Delft, The Netherlands (1996).

[10] Khan, Nisar Ali, Muhammad Fiaz Tahir, Camillo Nuti, Bruno Briseghella, and Alessandro Vittorio Bergami. "Influence of Brick Masonry Infill Walls on Seismic Response of RC Structures." Technical Journal 24, no. 03 (2019): 15-23.

[11] Vasconcelos, G., P. B. Lourenço, H. Mouzakis, and L. Karapitta. "Experimental Investigations on Dry Stone Masonry Walls." In 1st International Conference on Restoration of Heritage Masonry Structures, Cairo, Egypt, (2006):1-31.

[12] Manual, Abaqus User. "Abaqus Theory Guide. Version 6.14." USA: Dassault Systemes Simulia Corp (2014).

[13] Simulia, Dassault Systèmes. "Abaqus Analysis User's Guide, v. 6.14." Johnston, RI (2013).

[14] Deepak, Bansal. "Interlocking dry stacked masonry." In 8th International Masonry Conference. 2010.

[15] Belarbi, Abdeldjelil, L. X. Zhang, and THOMAS TC Hsu. "Constitutive laws of reinforced concrete membrane elements." In Sociedad Mexicana de Ingenieria Sismica in World Conference on Earthquake Engineering, pp. 1-8. (1996):1-8.

[16] Ghiassi, Bahman, Masoud Soltani, and Abbas Ali Tasnimi. "A Simplified Model for Analysis of Unreinforced Masonry Shear Walls Under Combined Axial, Shear and Flexural Loading." Engineering Structures 42 (September 2012): 396–409. doi:10.1016/j.engstruct.2012.05.002.

[17] Hibbitt, D., B. Karlsson, and P. Sorensen. "Abaqus/CAE user's guide." Dassault Systemes Simulia Corp., Providence, RI (2013).

[18] Prestandard, F. E. M. A. "commentary for the seismic rehabilitation of buildings (FEMA356)." Washington, DC: Federal Emergency Management Agency, 7, (2000).

[19] Senthivel, R., and P.B. Lourenço. "Finite Element Modelling of Deformation Characteristics of Historical Stone Masonry Shear Walls." Engineering Structures 31, no. 9 (September 2009): 1930–1943. doi:10.1016/j.engstruct.2009.02.046.

[20] Annecchiarico, M., F. Portioli, and R. Landolfo. "Micro and macro finite element modeling of brick masonry panels subject to lateral loadings." In Proc., COST C26 Action Final Conf, (2010):315-320.

[21] Rafiq, A. Computational Modelling of unconfined/Unreinforced Masonry Wall using Abaqus, MSc thesis, University of Engineering and Technology, Peshawar, Pakistan, (2016).

[22] Nikolić, Željana, Hrvoje Smoljanović, and Nikolina Živaljić. "Numerical modelling of dry stone masonry structures based on finite-discrete element method." International Journal of Civil, Environmental, Structural, Construction and Architectural Engineering 10, no. 8 (2016): 1032-1040.

[23] Safiee, N.A., M.S. Jaafar, and Jamal Noorzaei. "Behavior of Mortarless Wall Subjected to In-Plane Combine Loading." Advanced Materials Research 264–265 (June 2011): 1746–1751. doi:10.4028/www.scientific.net/amr.264-265.1746.

[24] Abdi, Rahim, and Nader Abdoli Yazdi. "Effects of Aspect Ratio and Plate Thickness on the Behavior of Unstiffened Steel-Plate Shear Walls with Pinned and Rigid Connections." Civil Engineering Journal 4, no. 6 (July 4, 2018): 1383. doi:10.28991/cej-0309180.

[25] Iuorio, O.; Fiorino, L.; Macillo, V.; Terracciano, M. T.; and Landolfo, R., "The Influence of the Aspect Ratio on the Lateral Response of the Sheathed Cold Formed Steel Walls". International Specialty Conference on Cold-Formed Steel Structures. 7, (2012).

[26] Kadhim, Jabbar Abdalaali, and Abbass Oda Dawood. "Seismic Performance of Clay Bricks Construction." Civil Engineering Journal 6, no. 4 (April 1, 2020): 785–805. doi:10.28991/cej-2020-03091508.